

fine (Tighnif) (30, 31), and especially Isenia (32–34).

The archaeological horizons are characterized by a great diversity in the frequencies of the various components (i.e., bifaces) and of waste types. This diversity likely reflects different hominin activities along the shores of the paleo-Hula Lake over time. The GBY lithic assemblages bear evidence of the presence of complex cognitive abilities (35) because the production of the desired tools entails design, dexterity, and flexibility.

Earlier evidence for hominin migration out of Africa is seen at 'Ubeidiya, with an Acheulean assemblage comparable to that from upper Bed II at Olduvai Gorge (~1.4 Ma). GBY provides evidence of a separate, chronologically younger, and culturally different entity, reflecting yet another human movement out of Africa. Lithic assemblages similar to those at GBY are unknown from contemporaneous sites in Eurasia. However, many technological patterns that make their first appearance outside Africa at GBY are characteristic of the later Eurasian record (36–41). Multidisciplinary investigations at GBY provide a unique opportunity to reconstruct the ecological background of hominin behavior during the early stages of human globalization.

References and Notes

1. O. Bar-Yosef and N. Goren-Inbar, *The Lithic Assemblages of 'Ubeidiya* (Qedem 34, Institute of Archaeology, Hebrew University, Jerusalem, 1993).
2. E. Tchernov, L. K. Horwitz, A. Ronen, A. Lister, *Quat. Res.* **42**, 328 (1994).
3. N. Goren-Inbar and I. Saragusti, *J. Field Arch.* **23**, 15 (1996).
4. W. Roebroeks and T. van Kolfschoten, in *The Earliest Occupation of Europe*, W. Roebroeks and T. van Kolfschoten, Eds. (Leiden University, Leiden, Netherlands, 1995), pp. 297–315.
5. M. Stekelis, *Bull. Res. Council Isr.* **G9**, 61 (1960).
6. E. Tchernov and D. Geraads, *L'Anthropologie* **87**, 138 (1983).
7. N. Goren-Inbar, S. Belitzky, Y. Goren, R. Rabinovitch, I. Saragusti, *Geoarchaeol.* **7**, 27 (1992).
8. N. Goren-Inbar et al., *Quat. Res.* **38**, 117 (1992).
9. N. Goren-Inbar, A. Lister, E. Werker, M. Chech, *Paleorient* **20**, 99 (1994).
10. N. Goren-Inbar and S. Belitzky, *Quat. Res.* **31**, 371 (1989).
11. A. Horowitz, *Isr. J. Earth Sci.* **22**, 107 (1973).
12. F. C. Bassinot et al., *Earth Planet. Sci. Lett.* **126**, 91 (1994).
13. E. Tchernov, *Cour. Forschungsinst. Senckenb.* **153**, 103 (1992).
14. W. von Koenigswald, O. Fejfar, E. Tchernov, *Neues Jahrb. Geol. Palaeontol. Abh.* **184**, 1 (1992).
15. J. Chaline and G. Farjanel, *Boreas* **19**, 69 (1990).
16. W. von Koenigswald and W.-D. Heinrich, *Kaupia* **9**, 53 (1999).
17. Y. Melamed, thesis, Bar Ilan University (1998).
18. D. L. Clark, *Analytical Archaeology* (Methuen, London, 1968).
19. G. L. Isaac, *Ologresallie, Archaeological Studies of a Middle Pleistocene Lake Basin, Kenya* (University of Chicago Press, Chicago, 1977).
20. \_\_\_\_\_, in *Stone Age Prehistory: Studies in Memory of Charles McBurney*, G. N. Bailey and P. Callow, Eds. (Cambridge University Press, Cambridge, 1986), pp. 221–241.
21. D. A. Roe, in (25), pp. 146–234.
22. \_\_\_\_\_, in (25), pp. 299–309.

23. P. Callow, in (25), pp. 235–253.
24. P. R. Jones, in (25), pp. 254–298.
25. M. D. Leakey and D. A. Roe, Eds., *Olduvai Gorge Excavations in Beds III, IV, and the Masek Beds 1968–1971* (Cambridge University Press, Cambridge, 1994).
26. J. D. Clark, in *After the Australopithecines: Stratigraphy, Ecology, and Culture Change in the Middle Pleistocene*, K. W. Butzer and G. L. Isaac, Eds. (Mouton, The Hague, 1975), pp. 605–659.
27. R. Potts, *J. Hum. Evol.* **18**, 477 (1989).
28. M. R. Kleindienst, *S. Afr. Arch. Bull.* **16**, 35 (1961).
29. J. D. Clark, *Am. Anthropol.* **8**, 202 (1966).
30. L. Balout, P. Biberson, J. Tixier, *L'Anthropologie* **71**, 217 (1967).
31. D. Geraads et al., *Quat. Res.* **25**, 380 (1986).
32. H. Roche, J.-P. Brugal, D. Lefèvre, S. Ploux, P.-J. Texier, *Afr. Arch. Rev.* **6**, 27 (1988).
33. H. Roche and P.-J. Texier, in *Evolution and Ecology of Homo erectus*, J. R. F. Bower and S. Sartono, Eds. (Leiden University, Leiden, Netherlands, 1995), pp. 153–167.
34. P.-J. Texier, in *La vie préhistoriques* (Faton, Dijon, France, 1996), pp. 58–63.
35. A. Belfer-Cohen and N. Goren-Inbar, *World Arch.* **26**, 144 (1994).
36. M. Santojna and P. Villa, *J. World Prehist.* **4**, 45 (1990).

37. W. Roebroeks, J. Kolen, F. Resnik, *Hellinium* **38**, 17 (1988).
38. A. Tuffreau, in *The Definition and Interpretation of Levallois Technology*, H. L. Dibble and O. Bar-Yosef, Eds. (Prehistory Press, Madison, WI, 1995), pp. 413–427.
39. A. Selkirk and W. Selkirk, *Curr. Anthropol.* **13**, 324 (1997).
40. M. Pitts and M. Roberts, *Fairweather Eden: Life in Britain Half a Million Years Ago as Revealed by the Excavations at Boxgrove* (Century, London, 1997).
41. M. B. Roberts and S. A. Parfitt, *Boxgrove: A Middle Pleistocene Hominid Site at Eartham Quarry, Boxgrove, West Sussex* (Archaeological Report 17, English Heritage, London, 1999).
42. Field work for this study was supported by the L. S. B. Leakey Foundation, the Irene Levi Sala Care Archaeological Foundation, the U.S.–Israel Binational Science Foundation, and the National Geographic Society. Laboratory analysis was supported by the Israel Science Foundation founded by the Israel Academy of Sciences and Humanities and by the Hebrew University, Jerusalem. We thank the GBY field crews (1989–1997) for their efforts. Figure 1 was created by G. Hivroni.

27 March 2000; accepted 5 June 2000

## A Single Adenosine with a Neutral pK<sub>a</sub> in the Ribosomal Peptidyl Transferase Center

Gregory W. Muth, Lori Ortoleva-Donnelly, Scott A. Strobel\*

Biochemical and crystallographic evidence suggests that 23S ribosomal RNA (rRNA) is the catalyst of peptide bond formation. To explore the mechanism of this reaction, we screened for nucleotides in *Escherichia coli* 23S rRNA that may have a perturbed pK<sub>a</sub> (where K<sub>a</sub> is the acid constant) based on the pH dependence of dimethylsulfate modification. A single universally conserved A (number 2451) within the central loop of domain V has a near neutral pK<sub>a</sub> of 7.6 ± 0.2, which is about the same as that reported for the peptidyl transferase reaction. In vivo mutational analysis of this nucleotide indicates that it has an essential role in ribosomal function. These results are consistent with a mechanism wherein the nucleotide base of A2451 serves as a general acid base during peptide bond formation.

During the early stages of model building on the 50S ribosome crystal structure, Moore, Steitz, and co-workers came to the anticipated, but hitherto unproven, conclusion that the peptidyl transferase center of the ribosome is composed exclusively of RNA (1, 2). Addition of peptidyl transferase inhibitors to the crystals led to the surprising observation that the nucleotide bases, rather than the phosphodiester backbone, are the components of the ribosome closest to the site of peptide bond formation (2). This suggested that the ribosome might catalyze protein synthesis using a nucleotide base as a general acid base, although the identity of the nucleotide was un-

known to us at the outset of these experiments.

Because none of the ribonucleotide functional groups in RNA have a pK<sub>a</sub> near the neutral pH that would be required for acid-base catalysis, we hypothesized that the pK<sub>a</sub> of an active site residue might be substantially perturbed in a manner analogous to that observed within protein enzymes and as proposed for the Hepatitis delta virus ribozyme (3–6). On the basis of the unperturbed pK<sub>a</sub> values of the nucleotide bases, the two most likely candidates for such an effect are the N1 of adenosine (A) and the N3 of cytidine (C), which have pK<sub>a</sub>'s of 3.5 and 4.2, respectively (7). Both of these functional groups can be methylated by dimethylsulfate (DMS) to produce a nucleotide adduct that terminates reverse transcriptase one nucleotide before the methylated base (8). A solvent-accessible residue with a neutral pK<sub>a</sub> should be unreactive to DMS modification at acidic pHs be-

Department of Molecular Biophysics and Biochemistry, Department of Chemistry, Yale University, 260 Whitney Avenue, New Haven, CT 06520–8114, USA.

\*To whom correspondence should be addressed. E-mail: strobel@csb.yale.edu

## REPORTS

cause of protonation, but as the pH is raised above the  $pK_a$ , the nucleobase would be deprotonated, resulting in increased DMS reactivity (9). Such a nucleotide could be readily distinguished from those with unperturbed  $pK_a$ 's because they would exhibit a constant level of DMS reactivity at all mildly acidic to basic pHs.

To validate this method, we measured the  $pK_a$  of 3-deazaadenosine (3dA), whose remaining N1 imino group has a spectrophotometrically determined  $pK_a$  of 7.0 (10). DMS was added to A or 3dA at pHs from 5.5 to 8.0, and the methylation rates were determined at each pH (11–13). The rate of DMS reactivity with A was constant at all pHs tested, consistent with its acidic  $pK_a$  (Fig. 1A). In contrast, the rate of 3dA methylation was markedly dependent on the pH of the solution (Fig. 1A). The log of the methylation rate was plotted versus pH to yield a calculated  $pK_a$  of  $6.4 \pm 0.1$ . This value is within half a pH unit of the spectroscopically determined value,

which was measured at substantially different ionic strength (10). This simple system demonstrates that DMS reactivity can be used to approximate a nucleotide's  $pK_a$ .

On the basis of this result, we performed DMS modification analysis on intact *E. coli* 50S ribosomal subunits in an attempt to identify the active site residue and measure its  $pK_a$  (14). The activity of the 50S subunits in the absence of methanol, intact tRNAs, or 30S subunits was confirmed with a modified form of the fragment reaction (15). The extent of DMS methylation at pHs from 4.5 to 8.6 was determined for each of the solvent-accessible A and C residues within domain V (nucleotides 2043 to 2625), which biochemical evidence suggests harbors the peptidyl transferase center (16). All residues throughout this region showed a similar level of DMS reactivity at all pHs tested, with the single exception of A2451 (Fig. 1B). This nucleotide was previously noted as having a weak DMS reactivity at pH 7.2 (17), but it is

almost fivefold more reactive at pH 8.0. This enhanced reactivity is dependent on the structural environment in the ribosome, as no pH dependent reactivity was observed in isolated and denatured 23S rRNA (18). The extent of A2451 DMS reactivity was plotted versus pH to give a calculated  $pK_a$  of  $7.6 \pm 0.2$  (Fig. 1C) (19). This value is within experimental error of the  $pK_a$  reported for the peptidyl transferase center based on the pH dependence of ribosome catalyzed peptide bond formation [ $7.7 \pm 0.3$  in (20) and  $7.3 \pm 0.1$  in (21)]. It corresponds to an increased basicity of more than 4 pH units relative to the unperturbed  $pK_a$  of adenosine.

Nucleotide A2451 is conserved in every living organism among all three biological kingdoms (22). It is located in the central loop of domain V and has been shown by DMS footprinting and photo-cross-linking experiments to be within the peptidyl transferase center (17, 23–26). Furthermore, within the completed 2.4 Å 50S structure, the base of A2451 (A2486 in *Haloarcula marismortui*) is immediately adjacent to the phosphoramidate analog of the tetrahedral intermediate (2). Thus, the sole nucleotide in the PTC that has a neutral  $pK_a$  is also in the best geometric position to catalyze protein synthesis.

There is some ambiguity in the interpretation of the DMS data regarding the site of A2451 modification. Within the 50S structure, the N3 of A2451 rather than the N1 is best positioned to act catalytically. This raises the following question: Which position of the base is DMS reactive and, by extension, which position has the perturbed  $pK_a$ ? In an unstructured RNA, DMS reacts to a greater extent with the N1 than with the N3 position of A (27), and it does not react at either position if the A is within a duplex (28). For these reasons, a reverse transcriptase stop at the nucleotide preceding an A (termed an n-1 RT stop) is usually taken as evidence for the N1 accessibility of a nucleotide (8), and it is possible that such is the case in the present study. However, the N3 of A is also susceptible to DMS modification, and it can be equally or more reactive than the N1 when it is presented in the right structural context (27). Model studies on N3-methyladenosine have shown that it is in equilibrium with the pyrimidine ring-opened *N*-(methylformamido)-imidazole derivative (29) (Scheme 1).

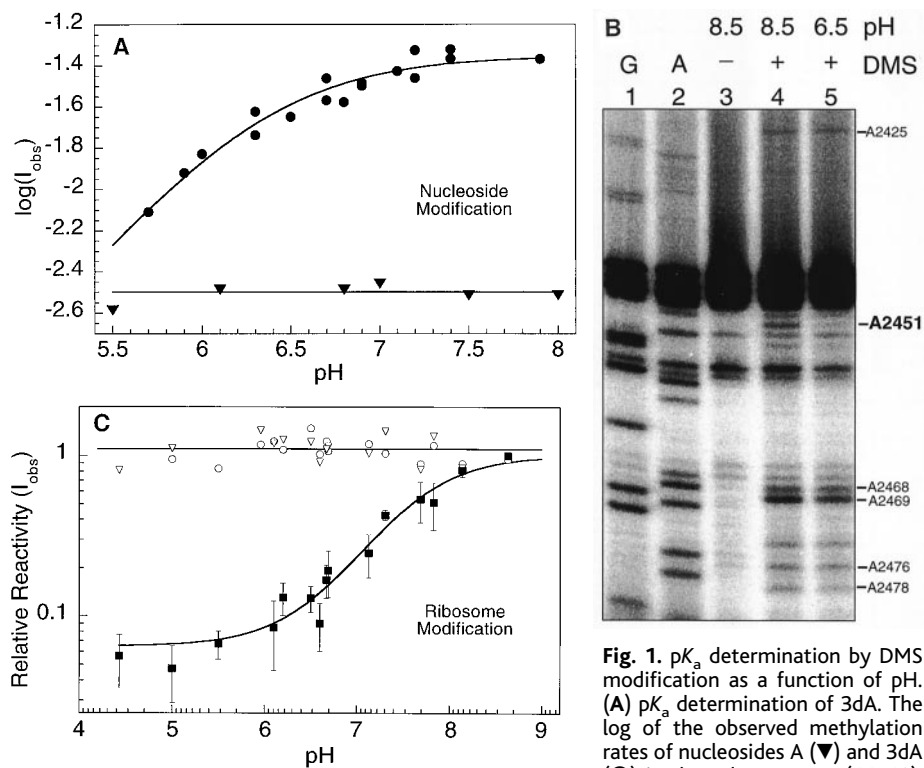
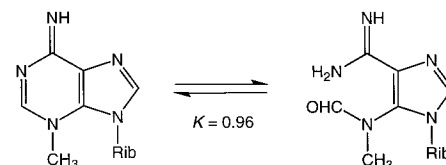


**Fig. 1.**  $pK_a$  determination by DMS modification as a function of pH. (A)  $pK_a$  determination of 3dA. The log of the observed methylation rates of nucleosides A ( $\blacktriangledown$ ) and 3dA ( $\bullet$ ) is plotted versus pH (11–13). Although the overall level of DMS

reactivity is greater for 3dA than A, only the 3dA reactivity changes as a function of pH. (B) A neutral  $pK_a$  of a single nucleotide within domain V of 50S ribosomes as measured by the pH dependence of DMS modification. Autoradiogram showing nucleotides 2425 to 2478 in domain V of *E. coli* 23S rRNA. Lanes 1 and 2, G and A dideoxy sequencing lanes, respectively. Lane 3, no DMS control of a 50S ribosomal subunit incubated in pH 8.5 buffer before RNA isolation and reverse transcription. Similarly, no DMS control lanes were run at all pHs tested, and no changes in band intensity were observed as a function of pH (18). Lanes 4 and 5, DMS modification of 50S ribosomal subunits at pH 8.5 and pH 6.5, respectively. pH-independent DMS modifications are observed at A2425, A2468, A2469, A2476, and A2478. Additional pH-independent modifications are observed at A2057, A2058, A2062, A2080, and A2247 (18). (C) Plot of the extent of DMS modification for three A's (A2468,  $\circ$ ; A2469,  $\nabla$ ; A2451,  $\blacksquare$ ) within the peptidyl transferase region of 50S ribosomal subunits as a function of pH (19). Each point is an average of five replicates at each pH, and the standard deviation is indicated with error bars.



**Scheme 1**

Either of these adducts could cause an n-1 RT stop, which suggests that DMS-induced transcriptional termination cannot be taken as un

## REPORTS

equivocal evidence for N1 modification of A.

Within the 50S active site cleft, the N3 of A2451 is solvent exposed, whereas the N1 is hydrogen bonded to the N1 of G2061 and does not appear to be accessible (2). There is nothing about the A2451-G2061 pair to suggest a pH dependence to its formation, and the positions of both bases are unchanged upon binding of peptidyl transferase inhibitors to the ribosome (2). If DMS reacts with the N1 of A2451 because of a pH-dependent conformational change in the active site, the N1 of G2061 is likely to become exposed to solvent. To explore this possibility, we used kethoxal, a reagent that reacts with the N1 and C2 amine of G to form a cyclic adduct that causes an n-1 RT stop (8). Previous mapping experiments on the 50S ribosome found that G2061 is not reactive with kethoxal at pH 7.2 (17), although the G2061 C2 amine is not hydrogen bonded and appears to be accessible within the active site cleft (2). We repeated the kethoxal experiment at pHs 6.5 and 8.5 and found that G2061 does not react with kethoxal at either pH (18). Although this is a negative result, it is consistent with the hypothesis that the N3 is the DMS reactive and chemically perturbed functional group of A2451. Because the N3  $pK_a$  of A could be at least 2 pH units lower than the N1, this result suggests that the  $pK_a$  shift in the ribosome active site may be as large as 6 pH units (30).

The functional importance of A2451 in the ribosome has not been investigated systematically. One early study reported that spontaneous mutation of A2451 to U in rat mitochondrial rRNA appeared to confer chloramphenicol resistance to 3T3 cells in culture, although no functional genetic test of the mutation was performed (31). We mutated A2451 to C, G, or U within the *rrnB* operon under the control of a temperature sensitive promoter (32). At 30°C, where the mutant rRNA is not expressed, *E. coli* containing either the wild type or any one of the three mutant plasmids grew equally well.

However, at 42°C, where the operon is expressed, all three mutant 23S rRNAs resulted in a dominant lethal phenotype (18). A plausible explanation for this result is that the assembly of peptidyl transferase-defective ribosomes onto polysomal messages is sufficient to block the activity of the wild-type ribosomes. Dominant lethality implies that A2451 is essential for ribosomal function.

A nucleotide base functional group with a  $pK_a$  of about 7.5 is well suited to act as both a general acid and a general base within the ribosome active site (Fig. 2). A base with such a  $pK_a$  can easily accept a proton (general base catalysis) from the nucleophilic amino group of the A-site-bound aminoacyl-tRNA during formation of the short-lived tetrahedral intermediate. An initial role as a general base is consistent with proton inhibition of the ribosomal fragment reaction at pHs below 9 [ $pK_i = 7.24$  ( $pK_i$  is the acid inhibition constant)] (21). After stabilizing the transition state, the adenosine could in turn transfer its proton (general acid catalysis) to the 3'-oxygen leaving group of the P-site tRNA as the tetrahedral intermediate is resolved into an amide linkage. In this way, A2451 may serve as a proton shuttle that acts in a manner analogous to that of the general acid-base residue in serine proteases (His<sup>57</sup> in chymotrypsin) (33, 34).

These results raise the obvious question: How does the RNA microenvironment in the peptidyl transferase center induce such a large shift in the A2451  $pK_a$ ? Our DMS mapping and mutagenesis data do not address this issue. The structure of the active site is discussed in the research article by Nissen *et al.* (2). They propose that two O6 carbonyls and a buried phosphate adjacent to the A2451 N6 might stabilize an alternative tautomeric form of the adenine base and/or create a charge relay system that substantially increases the basicity of the A2451 N3 (2).

Structural and biochemical data indicate that A2451 is the active site residue within the peptidyl transferase center. The universal

conservation of A2451 suggests that perturbation of its  $pK_a$  may have been a very early event in the evolution of biological catalysis. That this A may participate in the catalysis of peptide bond formation suggests that RNA achieved sophisticated mechanisms of transition state stabilization, including general acid-base catalysis, before the advent of templated protein synthesis.

### References and Notes

- N. Ban, P. Nissen, J. Hansen, P. B. Moore, T. A. Steitz, *Science* **289**, 905 (2000).
- P. Nissen, J. Hansen, N. Ban, P. B. Moore, T. A. Steitz, *Science* **289**, 920 (2000).
- G. J. Narlikar and D. Herschlag, *Annu. Rev. Biochem.* **66**, 19 (1997).
- A. R. Ferre-D'Amare, K. Zhou, J. A. Doudna, *Nature* **395**, 567 (1998).
- A. T. Perrotta, I. Shih, M. D. Been, *Science* **286**, 123 (1999).
- S. Nakano, D. M. Chadalavada, P. C. Bevilacqua, *Science* **287**, 1493 (2000).
- W. Saenger, *Principles of Nucleic Acid Structure* (Springer-Verlag, New York, 1984).
- S. Stern, D. Moazed, H. F. Noller, *Methods Enzymol.* **164**, 481 (1988).
- G. J. Connell and M. Yarus, *Science* **264**, 1137 (1994).
- N. Minakawa, N. Kojima, A. Matsuda, *J. Org. Chem.* **64**, 7158 (1999).
- Rates of DMS modification of A and 3dA (50 mM) were measured by dissolving the nucleosides in 25  $\mu$ l of 200 mM buffer containing 1/10 volume dimethyl sulfoxide (DMSO) at room temperature and adding 1  $\mu$ l of a 1:1 DMS/DMSO solution. Solutions were buffered with sodium cacodylate (pH 8.0 to 6.0) or sodium phosphate (pH 5.9 to 5.5). Aliquots (2  $\mu$ l) of the reaction were removed at various time points and quenched into 250  $\mu$ l of 200 mM KOH (pH 13). The change in ultraviolet (UV) absorbance (300 nm) of the quenched reaction was measured on a Cary 50 UV spectrophotometer and plotted versus time to calculate the reaction rate. The rate data were plotted versus pH and fit to Eq. 1 (12):

$$l_{\text{obs}} = \frac{l_{\text{max}} K_a}{K_a + [\text{H}^+]} \quad (1)$$

where  $l_{\text{obs}}$  is the observed DMS reaction rate at a given pH,  $l_{\text{max}}$  is the maximum rate of modification, and  $K_a$  is the equilibrium constant between the protonated and deprotonated form of the nucleoside.

- A. Fersht, *Enzyme Structure and Mechanism* (Freeman, New York, 1985).
- G. Fasman, *Handbook of Biochemistry and Molecular Biology. Nucleic Acids* (CRC Press, Cleveland, OH, ed. 3, 1975), vol. I. The product of the 3dA reaction with DMS (1-methyl-3dA) was isolated by reversed-phase high-performance liquid chromatography and characterized by <sup>1</sup>H nuclear magnetic resonance (NMR) and mass spectrometry (PerSeptive Biosystems Voyager-DE mass spectrometer). <sup>1</sup>H NMR ( $D_2O$ )  $\delta$  3.83 (s, 3H), 4.20 (m, 1H), 4.30 (m, 1H), 4.63 (m, 1H), 4.71 (m, 2H), 6.01 (d, 1H), 7.22 (d, 1H), 7.65 (d, 1H), 8.23 (s, 1H). MS calculated for  $C_{12}H_{17}N_4O_4^+$ : 281.125, found ( $m/z$ ) 280.164.
- Ribosomal subunits were isolated from early log phase *E. coli* MRE600 cells as described by H. J. Rheinberger, U. Geigenmüller, M. Wedde, and K. H. Nierhaus [*Methods Enzymol.* **164**, 658 (1988)]. 50S ribosomal subunits (1  $\mu$ M) were suspended in 50 mM buffer, 150 mM KCl, and 15 mM  $MgCl_2$  in a total volume of 50  $\mu$ l. RNA was methylated by adding 1  $\mu$ l of DMS diluted 1:10 in ethanol and incubating at 0°C for 1 hour. The solutions were buffered as follows: HEPES (pH 8.6 to 6.5); MES (pH 6.5 to 5.5); phosphate (pH 5.5 to 4.5). After isolation of the 23S rRNA by standard procedures, the sites of DMS modification within the rRNA were analyzed by primer extension with reverse transcriptase (avian myeloblastosis virus) with the 2493 5' end-labeled DNA primer (8, 17). Primers 2639, 2493, 2274, 2205, 2176, 2158, 2122, and 2101 were used to map the remainder of

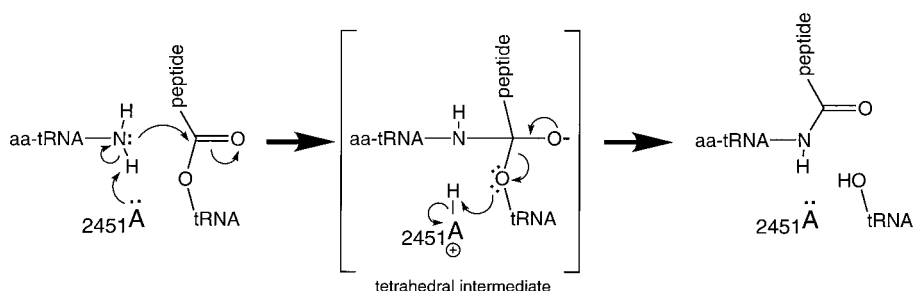


**Fig. 2.** Proposed general acid-base mechanism for ribosomal catalysis of the peptidyl transfer reaction. The details of the mechanism are discussed in the text. The lone pair of electrons shown on A2451 could be either those of the N1 or N3, although the N3 appears more likely on the basis of the crystal structure (2). The positive charge shown next to A2451 in the tetrahedral intermediate could reside on the base or be transferred to adjacent nucleotides by alternative tautomeric forms, as suggested by Nissen *et al.* (2).

domain V (18). Reverse transcription products were resolved by 6% denaturing polyacrylamide gel electrophoresis (PAGE), visualized, and quantitated with a Molecular Dynamics STORM PhosphorImager.

15. The A-site substrate 5' <sup>32</sup>P-labeled CACCPuromycin (1 μM) was reacted with CCA-Phe-Biotin (5 μM) in the presence of 50S subunits (2 μM) in buffer containing 10 mM tris HCl (pH 7.5), 100 mM NH<sub>4</sub>Cl, 30 mM MgCl<sub>2</sub>, and 4 mM β-mercaptoethanol at 37°C (18). Production of CACCPuromycin-Phe-Biotin was monitored as a function of time by PAGE to yield an observed rate constant of 0.03 min<sup>-1</sup> [B. E. H. Maden, R. R. Traut, R. E. Monro, *J. Mol. Biol.* **35**, 333 (1968)].

16. R. Green and H. F. Noller, *Annu. Rev. Biochem.* **66**, 679 (1997).

17. D. Moazed and H. F. Noller, *Cell* **57**, 585 (1989).

18. G. W. Muth, L. Ortoleva-Donnelly, S. A. Strobel, data not shown.

19. The DMS modification data were normalized for lane loading and extent of primer extension by dividing the peak area at each identified DMS-modified adenosine by the area of the intrinsic RT stop at nucleotides 2450 to 2447. These values were then normalized to a scale where maximum reactivity is defined as 1.0, by dividing the value for each adenosine by the value for the greatest extent of reaction (pH 8.6). The normalized modification data were fit to Eq. 2 (12):

$$I_{obs} = \frac{I_{HA} [H^+] + I_{max}}{K_a + [H^+]} \quad (2)$$

where  $I_{obs}$  is the observed extent of A2451 DMS modification at a given pH,  $I_{HA}$  is the extent of DMS reactivity for the protonated form of the nucleotide,  $I_{max}$  is the extent of reactivity for the deprotonated form of the nucleotide (defined as 1), and  $K_a$  is the equilibrium constant for protonation.

20. B. E. H. Maden and R. E. Monro, *Eur. J. Biochem.* **6**, 309 (1968).

21. S. Pestka, *Proc. Natl. Acad. Sci. U.S.A.* **69**, 624 (1972).

22. R. R. Gutell *et al.*, [www.rna.icmb.utexas.edu/CSI/fts.html](http://www.rna.icmb.utexas.edu/CSI/fts.html); R. R. Gutell, N. Larsen, C. R. Woese, *Microbiol. Rev.* **58**, 10 (1994).

23. D. Moazed and H. F. Noller, *Proc. Natl. Acad. Sci. U.S.A.* **88**, 3725 (1991).

24. P. Vannuffel, M. Di Giambattista, C. Cocito, *Nucleic Acids Res.* **22**, 4449 (1994).

25. D. Moazed and H. F. Noller, *Biochimie* **69**, 879 (1987).

26. G. Steiner, E. Kuechler, A. Barta, *EMBO J.* **7**, 3949 (1988).

27. P. Lawley and P. Brookes, *Biochem. J.* **89**, 127 (1963).

28. A. Maxam and W. Gilbert, *Proc. Natl. Acad. Sci. U.S.A.* **74**, 560 (1977).

29. T. Saito and T. Fujii, *J. Chem. Soc. Chem. Comm.* **1979**, 135 (1979).

30. The A N3 pK<sub>a</sub> has not been reported. A related nucleoside where the N3 pK<sub>a</sub> has been determined is 1-deazaadenosine (1dA), which has a single imino group in the six-membered pyrimidine ring (N3) with a pK<sub>a</sub> of 4.7 [F. Seela, H. Debelak, N. Usman, A. Burgin, L. Beigelman, *Nucleic Acids Res.* **26**, 1010 (1998)]. Removal of one of the two imino groups in the pyrimidine ring markedly increases the pK<sub>a</sub> of the remaining group. For example, the N1 pK<sub>a</sub> of 3dA is 7.0 ( $\Delta pK_a$  of +3.5 compared with A) (10), whereas the  $\Delta pK_a$  between pyridine and pyrimidine is +3.9 [from J. Lister, in *The Chemistry of Heterocyclic Compounds*, D. J. Brown, Ed. (Wiley, New York, 1971), pp. 448–453]. Assuming that the N3 of 1dA has a similar  $\Delta pK_a$  because of removal of the N1 imino group, the unperturbed pK<sub>a</sub> of A N3 would be about 4.7 – 3.7 = 1.0.

31. S. E. Kearsey and I. W. Craig, *Nature* **290**, 607 (1981).

32. A2451 was mutated to G, C, or U in the plasmid pLK35, which contains the rrnB operon under control of the bacteriophage λ P<sub>L</sub> promoter [S. Douthwaite, T. Powers, J. Y. Lee, H. F. Noller, *J. Mol. Biol.* **209**, 655 (1989)]. The mutant plasmids were transformed into pop2136 cells, an *E. coli* strain that expresses an integrated temperature sensitive form of λ repressor. In these cells, rrnB expression is induced at high temperature (42°C). Cells containing the wild type and three mutant plasmids were grown on 2xYT media containing 60 μg/ml of ampicillin at 30°C or 42°C.

33. J. Kraut, *Annu. Rev. Biochem.* **46**, 331 (1977).

34. T. Steitz and R. Shulman, *Annu. Rev. Biophys. Bioeng.* **11**, 419 (1982).

35. We thank A. Dahlberg for plasmid pLK35 and *E. coli* strain pop2136, B. Freeborn and A. Kosek for technical assistance, T. A. Steitz and P. B. Moore for information about the 50S structure before publication, D. M. Crothers and S. P. Ryder for helpful discussion,

and L. Weinstein, J. A. Doudna, A. A. Szwczak, and A. K. Oyelere for critical comments on this manuscript. This work was supported by a Basil O'Connor Award from the March of Dimes and NIH grant GM54839. G.W.M. is the recipient of an Anderson postdoctoral fellowship.

29 June 2000; accepted 24 July 2000

# Inhibition of Adipogenesis by Wnt Signaling

Sarah E. Ross,<sup>1</sup> Nahid Hemati,<sup>1</sup> Kenneth A. Longo,<sup>1</sup> Christina N. Bennett,<sup>1</sup> Peter C. Lucas,<sup>2</sup> Robin L. Erickson,<sup>1</sup> Ormond A. MacDougald<sup>1\*</sup>

Wnts are secreted signaling proteins that regulate developmental processes. Here we show that Wnt signaling, likely mediated by Wnt-10b, is a molecular switch that governs adipogenesis. Wnt signaling maintains preadipocytes in an undifferentiated state through inhibition of the adipogenic transcription factors CCAAT/enhancer binding protein α (C/EBPα) and peroxisome proliferator-activated receptor γ (PPARγ). When Wnt signaling in preadipocytes is prevented by overexpression of Axin or dominant-negative TCF4, these cells differentiate into adipocytes. Disruption of Wnt signaling also causes transdifferentiation of myoblasts into adipocytes in vitro, highlighting the importance of this pathway not only in adipocyte differentiation but also in mesodermal cell fate determination.

Adipocytes arise from mesodermal stem cells, which have the capacity to differentiate into a variety of other cell types, including myocytes (1). Once committed to the adipocyte lineage, preadipocytes can remain quiescent, multiply, or undergo differentiation and become adipocytes. 3T3-L1 and 3T3-F442A cells are established mouse preadipocyte models. Both cell lines can be induced to differentiate in cell culture, but 3T3-F442A cells are thought to be arrested at a later point in development (2). Studies of these cellular models have revealed some of the molecular events that orchestrate adipogenesis, including the role of C/EBPs and PPARγ in mediating the expression of adipocyte-specific genes (3, 4).

Wnts are a family of paracrine and autocrine factors that regulate cell growth and cell fate (5). Signaling is initiated when Wnt ligands bind to transmembrane receptors of the Frizzled family. In the canonical Wnt signaling pathway, Frizzleds signal through Dishevelled to inhibit the kinase activity of a complex containing glycogen synthase kinase 3 (GSK3), Axin, β-catenin, and other proteins. This complex targets β-catenin for rapid degradation through phosphorylation. Thus, once hypophosphorylated due to Wnt signaling, β-catenin is stabilized and translo-

cates to the nucleus where it binds the TCF/LEF family of transcription factors to regulate the expression of Wnt target genes (5–7).

To examine the role of Wnt signaling in adipogenesis, we tested whether Wnt expression in 3T3-L1 preadipocytes affected their ability to differentiate. We used Wnt-1 in these experiments because related cell lines, such as NIH-3T3 cells, respond to this ligand (8). In addition, we used two approaches to activate Wnt signaling downstream of the receptor: (i) treatment of cells with lithium, which inhibits GSK3 activity (9), and (ii) expression of a β-catenin mutant (β-catS33Y), which increases β-catenin stability (10). The 3T3-L1 preadipocytes were infected with a retrovirus vector alone (pLXSN) or retroviruses carrying either the genes for Wnt-1 (11) or β-catS33Y. After selection, cells were induced to differentiate in 10% fetal calf serum with methylisobutylxanthine, dexamethasone, and insulin (MDI). Control cells differentiated into adipocytes, as assessed by Oil Red-O staining and by immunoblot detection of the adipocyte fatty acid binding protein, 422/aP2 (12), whereas cells expressing Wnt-1 failed to differentiate (Fig. 1A). Neither lipid droplets nor 422/aP2 were detected in Wnt-1-expressing cells (12). Inhibition of differentiation was also observed when Wnt signaling was activated by lithium or β-catS33Y (Fig. 1A). Thus, Wnt signaling appears to inhibit adipogenesis in vitro.

Next, we used a model of adipocyte differentiation in which 3T3-F442A preadipocytes are injected subcutaneously into athymic mice (13, 14). Over several weeks, these

<sup>1</sup>Department of Physiology, <sup>2</sup>Department of Pathology, University of Michigan Medical School, Ann Arbor, MI 48109–0622, USA.

\*To whom correspondence should be addressed. E-mail: macdouga@umich.edu